Robotica (2016) volume 34, pp. 1822–1840. © Cambridge University Press 2014
doi:10.1017/S0263574714002598

Gait planning for a hopping robot

S. S. Shabestari† and M. R. Emami*‡

†*RWTH Aachen University, Aachen, Nordrhein-Westfalen, Germany*
‡*University of Toronto Institute for Aerospace Studies, Toronto, Ontario, Canada*

(Accepted October 13, 2014. First published online: November 26, 2014)

SUMMARY
An optimization model is developed in this paper for the joint trajectories of a hopping robot with a four-bar linkage leg. The dynamic behaviour of the one-legged robot is investigated during the stance and swing phases, and their impacts on gait planning are analysed. Certain constraints characterizing the continuous and cyclic motion of the robot are obtained. The optimization model is solved for the minimum torque and maximum velocity objective functions separately, and the results are compared with those in nature.

KEYWORDS: Legged robot; Hopping robot; Gait planning; Gait optimization; Motion planning.

1. Introduction

One legged hoppers were first designed to study the behaviour of the humanoid legged robots. The first studies on single-legged robots were initiated by Raibert in 1980s, based on the spring loaded inverted pendulum (SLIP) model.[1] Since then, he and his team at MIT have studied and prototyped various types of legged robots. Their single-legged robot was able to make stable hops in the sagittal plane using its hydraulically-actuated telescopic leg. The controls were decoupled in three PD controllers for the hopping height, forward velocity, and body attitude. The motion of the leg was assumed to be symmetric, meaning that the angle of the robot with respect to the ground at touch-down was the same as the angle at take-off. This type of motion was realized by designing trajectories using sinusoidal functions. The sinusoidal functions have the advantage of being simple and easy to generate, but they cannot be modified partially for specific objectives such as minimum impact at touch-down. The study of single-legged robots was then extended to a robot capable of 3D motion. Later on, Raibert and Thompson[2] showed that, with the use of two passive actuators and proper selection of initial conditions, it is possible to design a stable trajectory for a simple SLIP model making passive hops. Zeglin[3] developed a hopping robot, called Uniroo, which consisted of knee and ankle joints in addition to the hip joint and used a tail for balancing acts. The control and trajectory design were the same as those developed by Raibert. Buehler *et al.*[4] used the same approach to gait planning for their electrically-actuated hopping robot, called ARL. Through a detailed energy analysis, they were able to lower the electric actuation energy required for the autonomous locomotion. The robot followed a gait designed based on the Raibert's method. By the design of the ARL II, Buehler *et al.*[5] added a spring to the hip joint in order to passively store energy. It was shown that by using the proposed hip actuation, the robot could follow a trajectory close to its passive dynamic response. The desired gait trajectories were designed based on passive dynamic running motion of ARL II using a sinusoidal function.[6] Hyon and Mitta[7] developed a single-legged robot, Kenken, inspired biologically from dog's hind limb. The robot used two hydraulic actuators and a spring attached to the leg similar to the gastrocnemius. An empirical event-based controller was designed for the robot leading to successive planar hops. The gait that the robot followed during the swing phase was based on a modified sinusoidal function. During the stance phase, no trajectory design was required and the controller in this phase only ensured that the robot had enough energy for the next step. The robot was further modified by Hyon *et al.*[8] In Kenken IIR, a tail was attached to enhance its

* Corresponding author. E-mail: emami@utias.utoronto.ca

stability. The gait trajectory of the robot was improved using an optimization model based on an energy cost function. The designed trajectory was based on the Bezier function, and it was further refined using *poincáre* mapping. Vermeulen *et al.*[9] used Raibert's controller to study the effect of objective locomotion parameters and constraints in the gait design of a hopping robot. The objective locomotion parameters included the horizontal velocity of the centre of mass (CoM) of the robot, step length and step height. The trajectory was built using two polynomial functions. There were no conditions set on the velocity of the foot at touch-down, and therefore the impact of the robot to the ground was considered in the dynamic equations. The configuration of the robot at the beginning of each step and at certain instants was assumed to be known, and it was not part of the trajectory design. In his Ph.D. thesis, Vermeulen[10] applied the proposed trajectory design approach to other legged robot designs, such as a hopping robot with decoupled motion of upper body and leg, a hopping robot with a foot, a hopping robot with reduced ankle torque, a walking biped with instantaneous double support phase, and a walking biped with impact and double support phase. Guo *et al.*[11] proposed an optimization-based gait generation method applied to a single-legged robot model. The trajectory was designed through choosing the values of touch-down and take-off angles by trial-and-error. The values for the step length, height and forward velocity of the CoM during the swing phase were also given. The robot used the aid of a massless foot for more stability, and as a result the zero moment point (ZMP) criterion was added to the constraints of the optimization process. The objective function used in the optimization was based on the energy criterion, which resulted in the minimum energy input to the system. The gait was designed for two types of motion: hopping on even ground and upstairs. The same approach was applied to a biped model as well,[12] and the results indicated that the robot model was able to perform a human-like motion. Poulakakis and Grizzle[13] designed a hybrid controller that controlled the single-legged robot, THUMPER, equipped with a compliant transmission mechanism that had been developed by Hurst and Rizzi.[14] The controller acted on two levels. On the lower continuous level, the controller imposed virtual holonomic constraints on the dynamic system with the goal of restricting the motion of the robot to lower the dimensional surfaces. This *reduction by feedback* approach intended to make the robot behave as a hybrid zero dynamics (HZD) system. The upper event-based controller guaranteed that the robot made exponential stable hops following a nominal optimized gait. The energy criterion was used as the objective for the optimization and Bezier functions were used for trajectory planning. It was assumed that the robot would experience impact at touch-down instant by hitting the ground and at the take-off moment by the spring as it reaches its nominal length. Through further developments Grizzle *et al.*[15] applied the proposed control law to the biped robot, MABEL, using the same compliant transmission mechanism as the one used in THUMPER. Wu *et al.*[16] proposed an optimization procedure in order to design a trajectory for a single legged robot. The robot used the help of a flat foot to increase the stability. The trajectory was designed based on Bezier functions. The optimization objective was selected to be minimum torque input to the system. The resulting trajectory was then verified by simulation and hardware implementations.

While a few optimization approaches have been suggested in the literature to the design of gait trajectories for legged robots, as mentioned above, most of them assume certain given initial conditions and phase durations for the gait trajectory, which are either adopted from nature or based on the robot's structure. Further, little attention has been paid to reducing the leg impact at the touch-down moment as part of finding an optimum gait trajectory for hopping locomotion, which can significantly affect the structure design requirements. Moreover, further studies are needed for comparing optimized gait trajectories based on different objective functions and what can be found in nature for the locomotion of similar legged structures.

The goals of this paper are: **(i)** to develop a new optimization approach to the optimum gait trajectories for hopping robots by including the gait initial conditions and phase durations in the optimization process and by taking into account the elimination of the leg impact at touch-down; **(ii)** to implement the approach on the simulation model of a novel four-bar linkage mechanism for the hopping leg; and **(iii)** to evaluate the results by comparing the computed optimum gait trajectories with those in nature. The optimization approach includes the initial values of the robot configuration as the optimization variables along with the gait trajectory coefficients. Further, the proposed gait optimization also derives suitable values for the duration of each step and its characteristics, such as step height and length. The gait trajectory was optimized based on both energy and speed criteria. In Section 2, the geometry of the robot is described, and its motion phases and their corresponding

https://doi.org/10.1017/S0263574714002598 Published online by Cambridge University Press

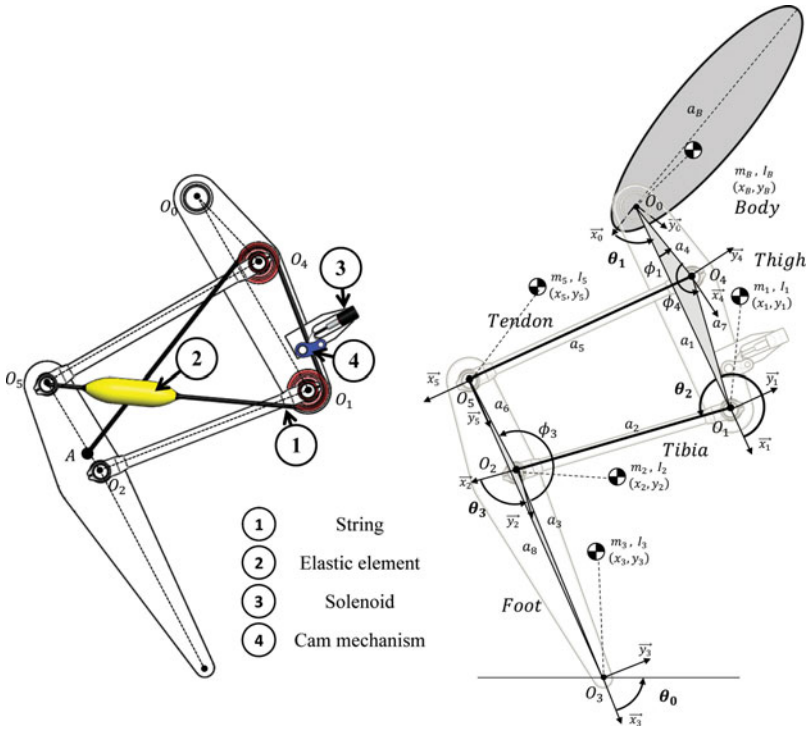

Fig. 1. Schematic model of the linkage leg.

dynamics are discussed. Section 3 details the system constraints for the gait optimization. In Section 4, objective functions are defined, and the optimization procedure is explained. The results are discussed in Section 5, followed by some concluding remarks in Section 6.

2. Dynamics of a Four-Bar Linkage Leg Robot

A new robot leg design has been introduced in,[17] which consists of revolute joints only and is capable of behaving similarly to a SLIP model during the stance phase and to a double pendulum model during the swing phase. The design, therefore, allows for a simple and intuitive method of understanding and defining the dynamics of the robot, as well as controlling it using the existing simpler control strategies for the SLIP and double pendulum. The robot consists of a single leg mechanism attached to a mass B representing the body (Fig. 1). The location of the CoM of the body does not coincide with the hip joint. This way the weight of the body introduces external momentum to the robot. This is a more complex design compared to the robots designed based on the SLIP model, where the CoM of the body is located at the hip joint and the leg is massless. The leg mechanism is a four-bar linkage. The first link is the thigh $\{O_0O_4O_1\}$ which is connected to the body at $\{O_0\}$; the second link is tibia $\{O_1O_2\}$, the third is foot $\{O_2O_3O_5\}$ and the fourth is tendon $\{O_4O_5\}$. The robot has two actuators connected at the hip joint $\{O_0\}$ and the knee joint $\{O_1\}$. The joints are actuated using electrical motors with gear transmission. The robot does not have a link resembling the human's foot, and it contacts the ground with just the toe $\{O_3\}$. The motion of the robot under study is characterized by stable and repeatable hops. Each hop consists of two consecutive phases, called stance and swing. During the stance phase, the robot is in contact with the ground at the toe $\{O_3\}$. It is also assumed that the ground is rigid to prevent the toe from penetrating through it, and the connection of the toe to the ground during the stance phase is fixed similar to a pivot joint with no external torque at the joint. These assumptions have also been made by other research works leading to real applications, e.g., [13] and [16]. Therefore, in the stance phase the robot has three degrees of freedom (DoF) parameterized by: the hip angle θ_1, Knee angle θ_2 and foot angle θ_0. Two of the joints are actuated, i.e., hip and knee, resulting in an under-actuated dynamics. In order to reduce the input energy to the system a spring is mounted between thigh and tibia. The spring can be locked (activated) and unlocked between the motion phases. The spring is activated in the stance phase to store energy during the first half of the

https://doi.org/10.1017/S0263574714002598 Published online by Cambridge University Press

motion and restore it into the system in the second half of the stance phase. Further details about the linkage leg mechanism have been discussed in.[17,18]

The linkage leg mechanism has a number of advantages over similar robotic legs. The leg employs only revolute joints, making it simpler to build and potentially lighter than legs with prismatic joints. The tibia and tendon segments are loaded only in compression and tension, respectively, making them easier to design and lighter to build. Further, the proposed linkage leg can change its knee angle at touch-down easily by changing the timing for locking the spring with no need for mechanical adjustments.

During the swing phase, the robot is completely in the air, and since the only external force acting on the robot is the gravitational force the CoM of the robot will follow a parabolic trajectory. Hence, in the swing phase the robot has five degrees of freedom parameterized by: the hip angle θ_1, knee angle θ_2, foot angle θ_0, the horizontal translation of the toe x_0 and the vertical translation of the toe y_0. Again, only hip and knee joints are actuated. The spring is unlocked (free) in this phase, so it does not store energy. One purpose of unlocking the spring is that spring vibrations from the previous stance phase do not affect the motion in the swing phase.

Considering q as the generalized coordinates, the motion of the robot can be described by Eq. (1):

$$M(q).\ddot{q} + C(q, \dot{q}).\dot{q} + g(q) = \tau + J(q)^T.f_g, \tag{1}$$

where M represents the inertia matrix, C is the matrix related to the Coriolis and centrifugal effects, and g defines the gravitational field vector. The matrix τ is the joint torque ($\tau = [\tau_{hip}\ \tau_{knee}\ [0]_{(1\times n)}]^T$), in which τ_{hip} and τ_{knee} are torque generated by the actuators at the hip and knee joints. The index n depends on the phase of motion, and can be 1 or 3 for the stance and swing phase, respectively. The vector $f_g = [F_g\ M_g]^T$ contains the interaction wrench (force and moment) between the robot and the ground, and $J(q)$ is the robot's Jacobian matrix.

Due to the transition of the DoF between the two phases of motion, two sets of q coordinates are defined as follows:

$$q_{st} = [\theta_1\ \theta_2\ \theta_0]^T, \tag{2}$$

$$q_{sw} = [\theta_1\ \theta_2\ \theta_0\ x_0\ y_0]^T, \tag{3}$$

The subscripts "st" and "sw" denote the stance and swing phase, respectively. During the swing phase, the reaction wrench of the ground, f_g, is zero. In the stance phase, the toe neither slides on the ground nor penetrates it. Therefore, the reaction wrench of the ground does not perform any work on the system. Hence, the robot can be considered as a fixed-base manipulator during the stance phase.

Optimizing the desired trajectories for the two actuators at the hip and knee joints requires complete knowledge of system DoF's during each phase. Before explaining how these are computed, some kinematic relations need to be obtained. By writing the kinematic equations in the linkage closed loop $\{O_1O_2O_5O_4\}$, the angles θ_3 and θ_5 can be calculated as functions of θ_2. Consequently, the angular velocities and accelerations of these two joints can be determined based on θ_2, its angular velocity, and its acceleration.

$$\theta_i = f_i(\theta_2), \tag{4}$$

$$\dot{\theta}_i = d_{i,2}.\dot{\theta}_2, \tag{5}$$

$$\ddot{\theta}_i = d_{i,2}.\ddot{\theta}_2 + \dot{d}_{i,2}.\dot{\theta}_2, \tag{6}$$

where $f_i(\theta_2)$ is the kinematic function relating θ_i ($i = 3, 5$) to θ_2, and $d_{i,2} = \frac{\partial\theta_i}{\partial\theta_2}$. (The explicit form of $f_i(\theta_2)$ is given in the Appendix.)

Being able to calculate θ_3 and θ_5 makes dynamic equations less complicated to solve. The number of degrees of freedom varies in each phase. In the following, the computation of inverse dynamics model for each phase is described.

https://doi.org/10.1017/S0263574714002598 Published online by Cambridge University Press

2.1. Stance phase

The system has three DoF's. The angles θ_1 and θ_2 are considered as actuated inputs and θ_0 is identified as the non-actuated variable. Therefore, the equations of motion can be rewritten as:

$$M(q_{st}).\ddot{q}_{st} + C(q_{st}, \dot{q}_{st}).\dot{q}_{st} + g(q_{st}) = \begin{bmatrix} \tau_{hip} \\ \tau_{knee} \\ 0 \end{bmatrix}. \tag{7}$$

The matrix relation (7) represents three equations. To determine the angle θ_0 and its derivatives, the third differential equation is solved first, using a numerical solver such as MATLAB's "ode45" function. Knowing θ_0, θ_1 and θ_2, the torque values τ_{hip} and τ_{knee} are then computed from the first two equations.

2.2. Swing phase

The system has five DoF's. Similar to the stance phase, the angles θ_1 and θ_2 are considered as actuated inputs. The foot angle θ_0, the horizontal translation of the toe x_0, and the vertical translation of the toe y_0 are the non-actuated variables. Therefore, the equations of motion can be rewritten as:

$$M(q_{sw}).\ddot{q}_{sw} + C(q_{sw}, \dot{q}_{sw}).\dot{q}_{sw} + g(q_{sw}) = \begin{bmatrix} \tau_{hip} \\ \tau_{knee} \\ 0 \\ 0 \\ 0 \end{bmatrix}. \tag{8}$$

The last three equations in the above matrix relation form a system of differential equations with three unknown variables, θ_0, x_0 and y_0. Therefore, they can be solved first using a numerical solver similar to the stance phase. The torque values τ_{hip} and τ_{knee} can be determined next by computing the first two equations in (8).

3. Constraints on the Hopping Motion of the Robot

Two main groups of constraints can be identified for the hopping motion of the single-legged robot:[24]

3.1. Instantaneous constraints

These are the constraints defined on a specific event or time instant.

3.2. Constraints on gait periodicity

To ensure a periodic motion a set of constraints need to be defined for the gait trajectory. Let us assume that the motion begins from the swing phase and ends with the stance phase. The final conditions of the robot are then defined as its conditions at the end of the stance phase. To ensure that the robot's gait is following a periodic trajectory, in each period the initial conditions of the swing phase must match the final conditions of the stance phase.

$$[\theta_1\ \theta_2\ \theta_0]_{sw,i} = [\theta_1\ \theta_2\ \theta_0]_{st,f} \tag{9}$$

$$[\dot{\theta}_1\ \dot{\theta}_2\ \dot{\theta}_0]_{sw,i} = [\dot{\theta}_1\ \dot{\theta}_2\ \dot{\theta}_0]_{st,f}. \tag{10}$$

The subscripts "i" and "f" denote the initial and final conditions of motion, respectively. Equations (9) and (10) also ensure that there will be a smooth transition from the stance phase to the swing phase.

3.3. Constraints on minimizing the impact

During the motion of robot, sudden changes of the DoF's and their derivatives will occur due to the phase transition. These changes are considered as physical impacts on the system, which cause energy dissipation. Without restoring energy into the system, the system cannot repeat its periodic motion. Therefore, the transition constraints ensure that there are no sudden changes in the DoF's despite

https://doi.org/10.1017/S0263574714002598 Published online by Cambridge University Press

the phase transition. A smooth transition between the two phases of motion is desirable for the gait trajectory; for this reason the initial values of the joint angles and their velocities for the stance phase is set equal to their final values in the swing phase. In addition, the initial value of the horizontal position of the toe is also set equal to its value at the end of the swing phase. This way the robot begins its stance at the same point where it landed on. The initial value of the vertical displacement of the toe for the stance phase is known to be zero. As a result, the desirable final value of this variable during the swing phase should also be zero. This can be realized by introducing the condition:

$$y_{0_{sw,f}} = 0. \tag{11}$$

To smooth the changes in the rate of DoF's, animals tend to retract their leg prior to touch-down. In legged locomotion, as shown by Seyfarth *et al.*[21] and Wisse *et al.*,[22] leg retraction prior to touch-down helps the motion periodicity. Therefore, by reducing the absolute velocity of the toe with respect to the ground one would be able to eliminate the impact effects. The above arguments can be summarized as:

$$[\dot{x}_0 \ \dot{y}_0] = [0 \ 0]. \tag{12}$$

3.4. Constraints on numerical computations

Depending on the initial conditions, the ODE solver may not converge to a solution or may give unrealistic solutions. In such cases, the solver should be stopped and the computed data should be discarded by the optimizer. In order to prevent the optimizer from refining these solutions, a binary variable, namely error flag, is defined and included in the constraints. As there are two sets of ODE computations for the swing and stance phases, one error flag is defined for each phase. The error flags look for special events during the ODE computations. For the swing phase, these events can be defined as:

- The duration of solving the differential equations is more than a threshold (e.g., 5 s).
- The vertical position of the hip joint O_0 is negative or bigger than a threshold (e.g., 3 m). In such cases, the robot either goes into the ground or flies in the air, which are unrealistic and cause the optimizer to have large number of iterations unnecessarily.
- The vertical position of the toe is out of a predefined range (e.g., bigger than -1 m and less than 1 m). In these solutions the robot has an unrealistic rotation, and again the ODE solver does not need to continue.

For the stance phase, the first two of the above events are checked as the toe is positioned stationary on the ground.

3.5. Permanent inequality constraints

The second group of constraints include those that must be held during the entire period or a portion of the motion.

3.5.1. Unilateral contact condition. This constraint implies that at any time during the motion, the leg cannot penetrate into the ground. During the swing phase, this constraint ensures that the combination of expansion and rotation of the leg does not lead to the collision to the ground. During the stance phase, the constraint prevents the toe from penetrating the ground level. In this work, during the swing phase the constraint is defined as:

$$y_{0,min} > 0. \tag{13}$$

During the stance phase, such a constraint is applied through the derivation of the equations of the motion by setting the value of y_0 to zero in this phase. This means that, based on the derived mathematical equations, only the motions in which the robot stays on the ground would be considered for the optimization.

https://doi.org/10.1017/S0263574714002598 Published online by Cambridge University Press

3.5.2. Non-sliding condition. This constraint applies only to the stance phase. It is assumed that during the stance phase the friction force applied to the toe is large enough to prevent slipping of the toe on the ground. The constraint is applied to the mathematical equations of motion by putting x_0 to zero during stance phase and by ensuring that at each instant of the stance phase, the ratio of the horizontal component to the vertical component of the ground reaction force does not exceed the surface static friction coefficient μ.

$$\frac{\mid (F_g)_{horizontal} \mid}{(F_g)_{vertical}} < \mu. \tag{14}$$

3.5.3. Internal and external non-collision constraints. The self-collision of internal components of the robot leg must be avoided at all times. The same condition applies to the external collision with the obstacles, in this case the ground. To prevent the self-collision, the actuated joint movements should be limited. Consequently, the limitations of the movements for the hip and knee joints are defined as follows. (ϕ_1 is shown in Fig. 1.)

$$-\pi < \theta_1 < \pi - \phi_1, \tag{15}$$

$$\pi < \theta_2 < 2\pi. \tag{16}$$

As for the external collision, the non-actuated joint θ_0 is limited during the stance phase. This will prevent any point of the robot, other than toe, from contacting the ground. Hence, the defined range for θ_0 is as follows:

$$\pi/4 < \theta_0 < 3\pi/4. \tag{17}$$

3.5.4. Motion dependent constraints. Certain behaviours of the robot are not acceptable, and the optimizer is notified about them through the following constraints:

$$\dot{x}_{CoM} > 0, \tag{18}$$

$$(\dot{y}_{CoM})_{sw,i} > 0, \tag{19}$$

$$(y_{O_0})_{st,f} > 0. \tag{20}$$

Using Eq. (18) as a constraint prevents the backward motion of the CoM of the robot during the entire step. The robotic leg must also have a positive vertical velocity at the take-off moment (initial condition of the swing), Eq. (19), otherwise it may penetrate into the ground. The constraint (20) checks the vertical position of the hip at the end of stance phase (take-off moment) to be always positive.

3.5.5. Impact torque constraints. There is a sudden change of torque at the hip and knee joints when the robot hits the ground at touch-down. For practical purposes, this change should remain less than a maximum value for the actuators and the controller to be able to handle the load quickly. This condition will introduce the following two constraints to the optimization model:

$$\mid (\tau_{hip})_{sw,f} - (\tau_{hip})_{st,i} \mid < \Delta\tau_{hip}, \tag{21}$$

$$\mid (\tau_{knee})_{sw,f} - (\tau_{knee})_{st,i} \mid < \Delta\tau_{knee}, \tag{22}$$

where $\Delta\tau_{hip}$ and $\Delta\tau_{knee}$ are the maximum allowable change of torque at the hip and knee joints, respectively.

3.5.6. Maximum torque constraints. To ensure that the optimum gait trajectories do not require excessive torque at the hip and knee joints beyond the capacity of the assigned actuators, the following

https://doi.org/10.1017/S0263574714002598 Published online by Cambridge University Press

constraints are defined:

$$| \tau_{hip} |_{max} < \bar{\tau}_{hip}, \tag{23}$$

$$| \tau_{knee} |_{max} < \bar{\tau}_{knee}, \tag{24}$$

where $\bar{\tau}$ is the maximum allowable torque at the hip and knee joints.

3.5.7. Trajectory stability. One of the issues in studying legged locomotion is how to define a stable trajectory and relate it to the system dynamics. The gait stability of a legged locomotion can be realized using stability margins such as: eigenvalues of the *poincáre* return map, change of the angular momentum, and the ground reference points.[20] A mathematical definition of the stability is given in,[19] based on which as long as a legged robot is not in the basin of fall the motion is considered to be stable. The basin of fall is a "subset of the state space that leads to a *fall*, (where) a point on the robot, other than a point on the foot, touches the ground." Based on these definitions, a continuous periodic motion can be stable if and only if in each period the robot does not fall. As a result, in addition to Eqs. (9) and (10) which define the gait periodicity, the constraint defined in Eq. (17) along with those for the numerical computation will ensure that the robot does not fall during each period. Once an optimum periodic gait is found by which the robot does not fall during a period of motion, it can be said that the robot trajectory is stable.

4. Optimization Procedure

Two major objectives are usually considered independently for the optimization of hopping robots: minimum overall consumed energy and maximum forward velocity.

For the energy-based objective, a sthenic criterion is selected,[24] which minimizes the total input torque to the joints. The total consumed torque is divided by the step length to prevent the optimizer from selecting the shortest hopping distance per a single hop as the optimum solution, since in a motion consisting of several hops the one with the shortest hops is not necessarily the least energy consuming solution. Therefore, the torque-based objective function, to be minimized, has the form of:

$$J = \frac{1}{d_{x,CoM}} . \int_{t_i}^{t_f} (\tau_{\text{hip}}(\text{t})^2 + \tau_{\text{knee}}(\text{t})^2)\, \text{d}t, \tag{25}$$

where $\tau(t)$ is the torque applied at the hip and knee joints and $d_{x,CoM}$ is the horizontal distance travelled by the CoM.

The second objective function, to be maximized, is the forward (horizontal) velocity. Though this objective can be expressed by the velocity of the hip, toe, body or robot CoM, the latter is selected here since it directly relates to the robot forward velocity and can be compared with other legged robots as well as humans. The objective function consequently has the form of:

$$J = min(V_{x,CoM})_{cycle}. \tag{26}$$

The horizontal velocity of the CoM is not constant in each step, especially during the stance phase. In order to have an objective function indicating the velocity of the robot for the entire step, the minimum value of the horizontal velocity of the CoM is selected. By maximizing this value, the maximum speed of the robot can be found given the defined torque range and other constraints.

The optimization constraints vary depending on the objective function. For the torque-based optimization using (25), there are 11 equality constraints, namely Eqs. (9)–(12) and the two error flags, as well as 10 inequality constraints, namely those in Eqs. (13)–(24). For the velocity-based optimization, there are two additional inequality constraints related to the maximum allowable torque applied to the two actuated joints.

The goal of the optimization is to find the best profiles for the angles θ_1 and θ_2 representing the relative displacement of the actuated hip and knee joints, respectively, so that either of the above-mentioned objective functions is extremized given the motion and power constraints. Therefore, two functions are required for calculating the trajectory of θ_1 and θ_2 during each cycle. Several functions

https://doi.org/10.1017/S0263574714002598 Published online by Cambridge University Press

Table I. Optimization variables.

Name	Variable
θ_1 Bezier coefficients for the swing phase	$[x_1\ x_2\ x_3\ x_4\ x_5\ x_6]_{\theta_1,sw}$
θ_2 Bezier coefficients for the swing phase	$[x_1\ x_2\ x_3\ x_4\ x_5\ x_6]_{\theta_2,sw}$
θ_1 Bezier coefficients for the stance phase	$[x_1\ x_2\ x_3\ x_4\ x_5\ x_6]_{\theta_1,st}$
θ_2 Bezier coefficients for the stance phase	$[x_1\ x_2\ x_3\ x_4\ x_5\ x_6]_{\theta_2,st}$
Initial values of θ_1 , θ_2 and θ_0	$[\theta_1\ \theta_2\ \theta_0]_{sw,i}$
Initial values of $\dot{\theta}_1$, $\dot{\theta}_2$ and $\dot{\theta}_0$	$[\dot{\theta}_1\ \dot{\theta}_2\ \dot{\theta}_0]_{sw,i}$

are used in the literature for the joint trajectory profile, including sinusoidal, polynomial and Bezier functions. The Bezier function has some useful features as it exhibits smooth curves and does not show large oscillations with small parameter perturbations, which is advantageous in numerical computations.[23] A typical Bezier function can be defined as:

$$\theta(t) = \sum_{i=0}^{m} \frac{m!}{i!(m-i)!} t^i (1-t)^{m-i} . x_i, \tag{27}$$

where m is the order of the polynomial and x_i are characterizing weighting coefficients, called Bezier coefficients. As a result, the Bezier coefficients of their corresponding trajectories are the optimization variables. Further, the trajectory of each joint is highly dependent on the initial posture and velocity of the robot. Therefore, such motion initial conditions are also included in the optimization variables.

Since each of the swing and stance phases exhibits a different dynamic behaviour, it is more practical to find two separate sets of joint trajectories for the swing and stance phases, which satisfy the transition conditions between the phases. Therefore, four sets of Bezier coefficients, two for each joint, are to be designed. The gait optimization problem of the single-legged hopping robot is then solved by finding the Bezier coefficient sets and motion initial conditions to minimize the torque-based objective function (25) or maximize the velocity-based objective function (26) under the equality constraints (9)–(12) and inequality constraints (13)–(24). The optimization variables are given in Table (I).

Each iteration step of the optimization begins by computing the DoF's for the swing mechanism. First, the actuated DoF's are calculated from (27) having the optimization variables including Bezier coefficients for each joint trajectory and the initial conditions for the joints angular positions and velocities. Then, the under-actuated DoF's are determined by solving the set of differential equations included in (8), using the MATLAB function $ODE45$. Next, the state of the system is known and the required torque can be calculated using the inverse dynamics equations of (8). Similar steps are repeated for the stance phase using (7). In order to have a smooth transition between the two phases, the initial conditions of the stance phase are set equal to the final state of the swing phase. The optimization procedure is summarized in the flowchart shown in Fig. (2). For solving optimization numerically the MATLAB function $fmincon$ was used.

One important parameter in optimizing the motion of the robot is the duration of each phase, which is a function of optimization variables. The duration of the swing phase in each iteration can be computed based on the touch-down event, that is when the vertical position of the toe crosses zero and the ODE solver for the swing phase is terminated. However, it was discovered that this mechanism can cause the optimization to have difficulty satisfying condition (12). This is due to the expected action of the toe at the end of the swing phase. The constraint (12) requires the toe to have zero absolute velocity at the end of the swing phase. Given the motion of the robot CoM at the end of the swing phase, the toe should have a back-and-upward relative motion at this instant. To facilitate this, in some iterations the toe needs to move toward and into the ground and then at the end of the swing phase it moves out of the ground. Although such solutions are physically impractical, they help the optimizer to further refine the iterations towards physically viable solutions with zero absolute velocity for the toe at the end of the swing phase. Based on the above reasoning, It would be more

https://doi.org/10.1017/S0263574714002598 Published online by Cambridge University Press

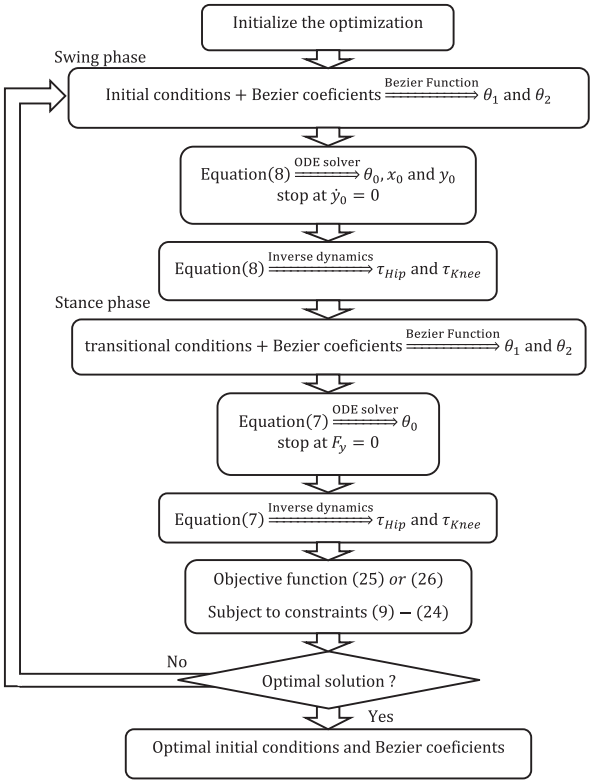

Fig. 2. The optimization procedure flow chart.

effective for the optimization to check for the vertical velocity of the toe for ending the ODE solver and, hence, finding the duration of the swing phase.

The optimization requires an initial guess for the duration of the swing phase to solve for the differential equations numerically. The initial guess is set to be the maximum allowable duration of the swing phase, which can be calculated based on the maximum allowable vertical displacement of the robot CoM, as shown in Eqs. (28) and (29):

$$T_{sw,max} = 2.V_{y.CoM,max}/g, \tag{28}$$

$$V_{y.CoM,max} = \sqrt{2.\Delta Y_{CoM,max}.g.} \tag{29}$$

The duration of stance phase in each iteration, can be computed based on take-off event, that is when the ground vertical reaction force crosses zero and the ODE solver for the stance phase is terminated. Similar to the swing phase, a maximum allowable duration is given as the initial guess for the optimization of the stance phase.

5. Discussion of Results

The optimization procedure described in the previous section is applied to a model of the single-legged hopping robot designed in.[17] The geometric and dynamic parameters are listed in Table (II).

The spring attached to thigh and tibia is assumed to be massless with stiffness of 65 KN/m. The spring can be activated using a special locking mechanism. The free length of the spring is selected to be its length at the beginning of the stance phase.

The order of the Bezier functions used for the joint trajectories has to be selected in a way to satisfy all of the constraints. Due to the large number of constraints, the order of the Bezier function is set to 8.

The results of the optimization process for each objective function are discussed in the following:

https://doi.org/10.1017/S0263574714002598 Published online by Cambridge University Press

Table II. Geometric and dynamic parameters of the single-legged robot.

			Thigh			
Length$[m]$/angle$[rad]$	a_1	0.5	a_4	0.202	ϕ_1	0.237
Mass$[kg]$	m_1	0.567				
Moment of inertia$[kg.m^2]$	I_1	0.02				
$X_{CoM}[m]$	x_1	0.0				
$Y_{CoM}[m]$	y_1	0.123				
			Foot			
Length$[m]$/angle$[rad]$	a_3	0.5	a_6	0.230	ϕ_3	3.206
Mass$[kg]$	m_3	0.673				
Moment of inertia$[kg.m^2]$	I_3	0.01				
$X_{CoM}[m]$	x_3	0.5				
$Y_{CoM}[m]$	y_3	0.057				
	Body		**Tibia**		**Tendon**	
Length$[m]$	a_B	0.5	a_2	0.5	a_5	0.548
Mass$[kg]$	m_B	18	m_2	0.38	m_5	0.237
Moment of inertia$[kg.m^2]$	I_B	1.5	I_2	0.013	I_5	0.022
$X_{CoM}[m]$	x_B	0.2	x_2	0.232	x_5	0.476
$Y_{CoM}[m]$	y_B	0.01	y_2	0.133	y_5	0.153

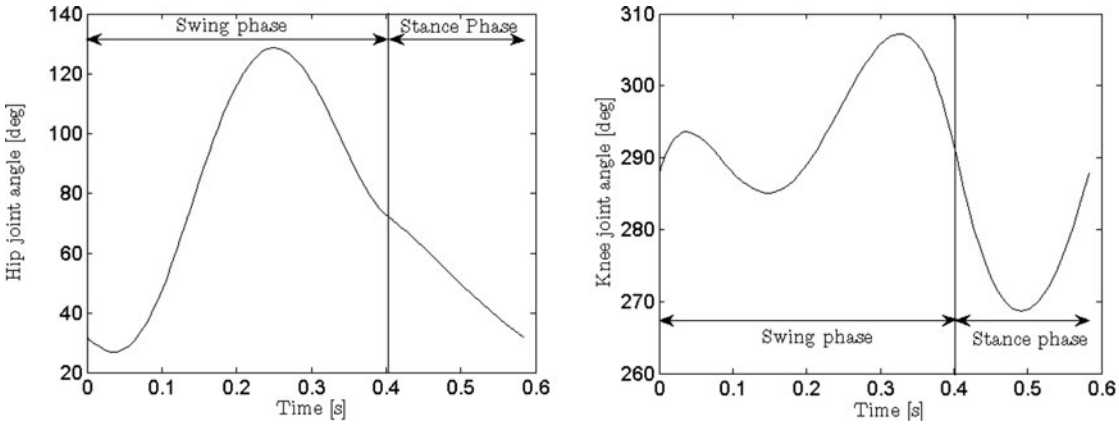

Fig. 3. Optimal trajectory for the actuated joints during one step.

5.1. Minimum input torque

The optimized trajectories of the actuated joints and their velocities are given in Figs. (3) and (4). In the beginning of the swing phase the knee angle is increasing, meaning that the leg is extending. This is expected because the knee joint has a positive angular velocity at the end of the stance phase. Therefore, the condition for the continuity of the joint angular velocity necessitates that the knee joint starts the swing phase with a positive velocity resulting in extending the leg. Note that in this example, there is no restriction on the continuity of the joint acceleration (or torque). To accommodate the leg extension in the beginning of the swing phase without causing the toe to hit the ground, the leg needs to rotate backward. This is accomplished by rotating the hip joint backward (decreasing the joint angle), because in this period the body orientation is still nearly stationary due to its larger moment of inertia relative to the leg. After this short period in the swing phase, the hip joint angle increases as both the leg and body rotate forward, until a certain point where the hip joint should rotate backward again to bring the absolute velocity of the toe to zero at touch-down while the leg is retracting. It is also noted that the leg goes through two cycles of extension–retraction during the swing phase. This is because the knee needs to retract in the middle of the swing phase to prevent the toe from hitting the ground.

https://doi.org/10.1017/S0263574714002598 Published online by Cambridge University Press

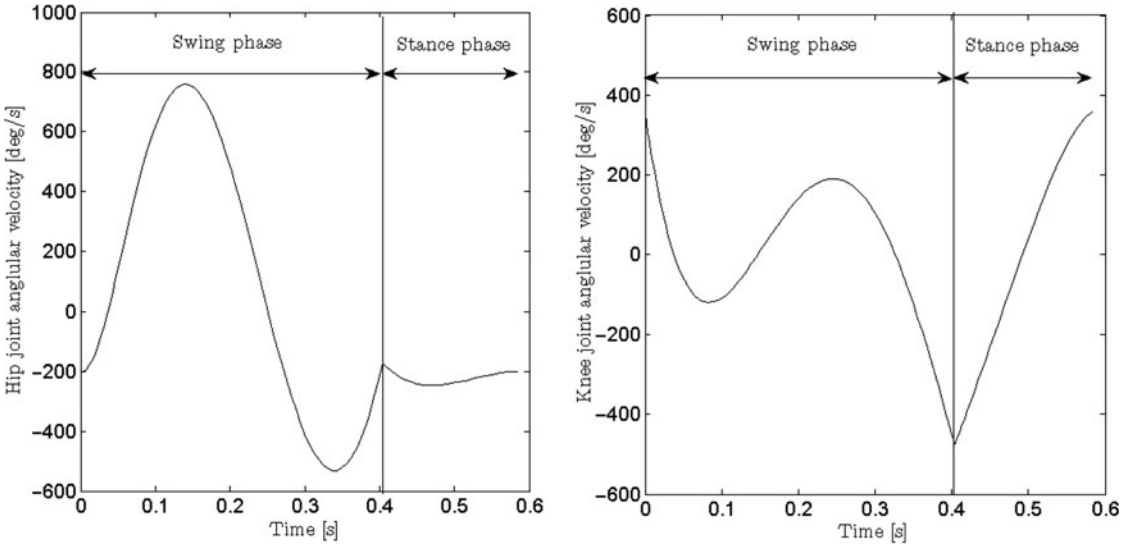

Fig. 4. Angular velocity of the actuated joints during one step.

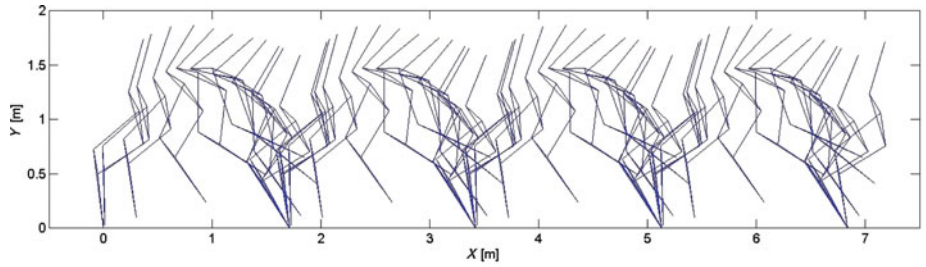

(a) Four steps of the motion

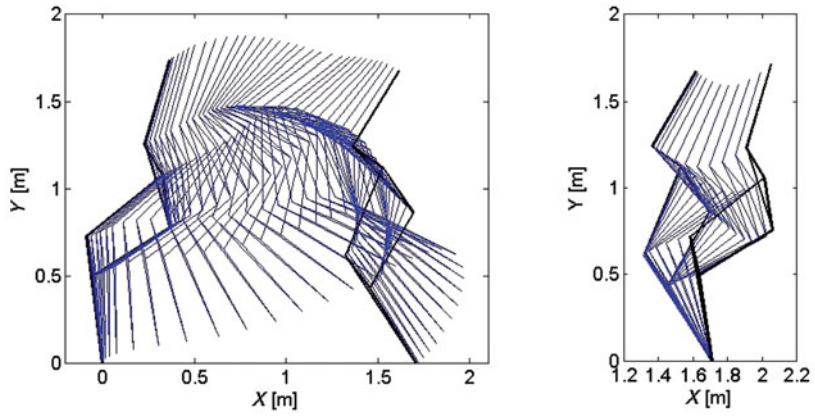

(b) Swing phase (c) Stance phase

Fig. 5. Stick diagram of the robot motion during each phase of motion. (a) Four steps of the motion. (b) Swing phase. (c) Stance phase.

During the stance phase, the leg continues to retract until a certain point where the leg extension should begin to help the robot gain the required velocity for the next swing phase. The motion of the robot during each phase is illustrated in Fig. (5).

The optimum torque at the actuated hip and knee joints during each phase is given in Fig. (6). The jump in the torque at the phase shift, is due to the change in the dynamic behaviour of the robot in which right after touch-down the ground reaction forces act on the robot. The jump in the

https://doi.org/10.1017/S0263574714002598 Published online by Cambridge University Press

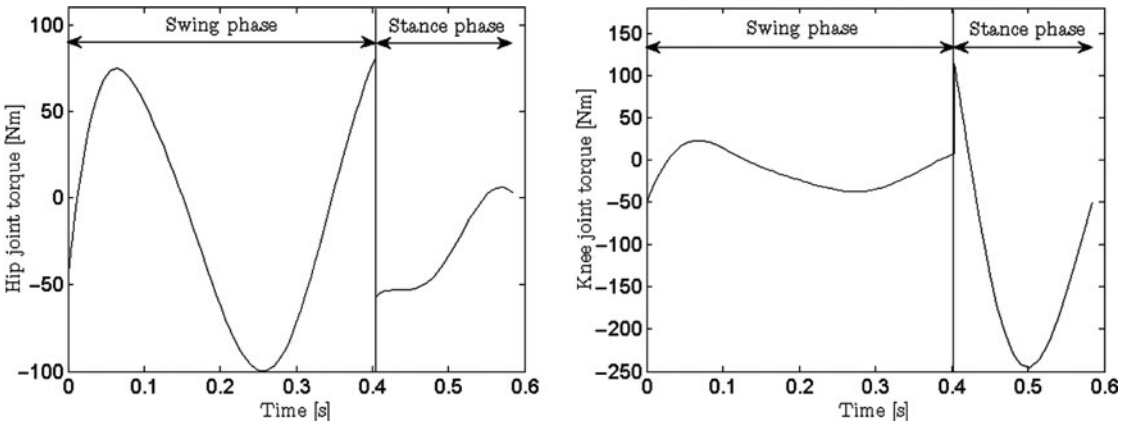

Fig. 6. Input torque of the actuated joints.

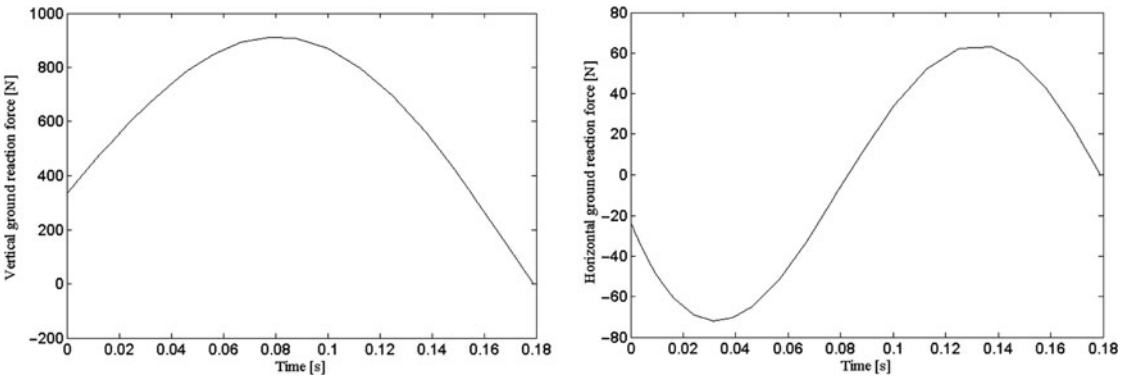

Fig. 7. Ground reaction forces during the stance phase.

torque values at the transition point is due to the sudden introduction of the ground reaction force at touch-down. The change must be less than a maximum value, as dictated by constraints (21) and (22), to enable the actuator (and controller) to follow the optimum trajectory. The maximum change of torque for both hip and knee actuators was considered as $350Nm$ for this work, which is a typical value in similar research works [1 and 25]. Therefore, the jumps in Fig. (6) are well below the limit. The maximum input torque occurs during the stance phase through the leg retraction. This is due to the high stiffness of the spring attached to the leg, which means the leg's momentum alone is not sufficient for compressing the spring to store energy and additional input torque is needed from the knee joint actuator, as shown in Fig. (6). The ground reaction forces during the stance phase are plotted in Fig. (7). The highest reaction force occurs at the end of the stance phase when the toe takes off the ground. However, the ratio of the horizontal to vertical reaction forces is still quite small (0.16). Therefore, to avoid slippage the static friction coefficient between the toe and the ground surface needs to be larger than 0.16.

5.2. Maximum velocity

The optimization procedure with the objective of maximum horizontal velocity of CoM requires a limit on input torque. The torque range is selected to be within $-350Nm < \tau < 350Nm$ for each joint, which is a trade-off between limiting the required power yet allowing the leg to reach high velocities. Higher motor power results in larger and heavier motors and power supplies. The optimized angular trajectories of the actuated joints and their speeds are given in Figs. (8) and (9), and the motion of the robot during each step is illustrated in Fig. (10). The resulting trajectories have the same trend as those of the minimum torque optimization. This is due to the fact that the hopping nature of the motion has remained the same for both cases. The maximum velocity of CoM is realized by increasing the jump distance and decreasing the jump height during the swing and decreasing the

https://doi.org/10.1017/S0263574714002598 Published online by Cambridge University Press

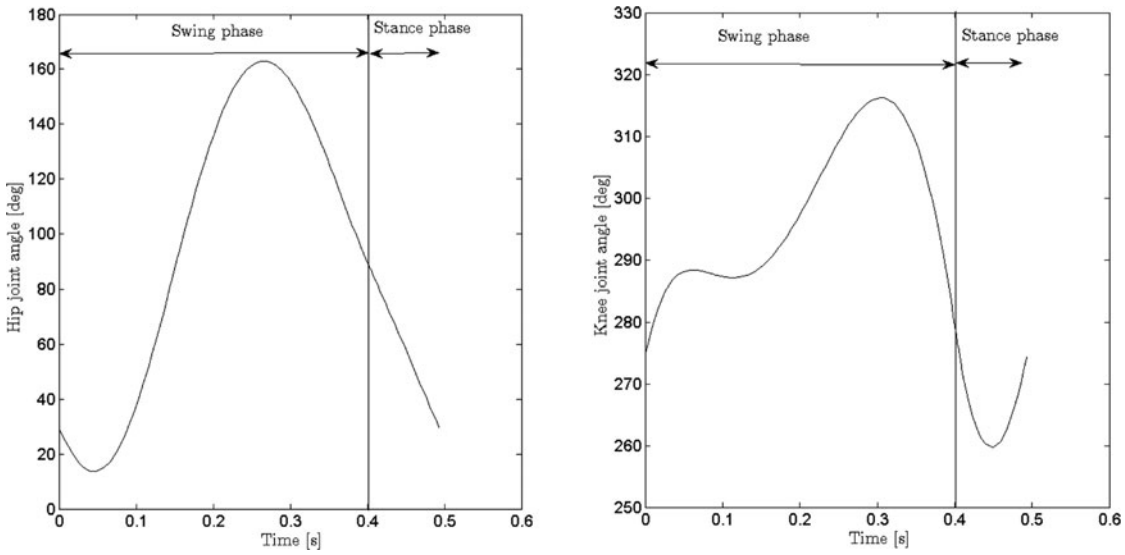

Fig. 8. Optimal trajectory for the actuated joints during one step.

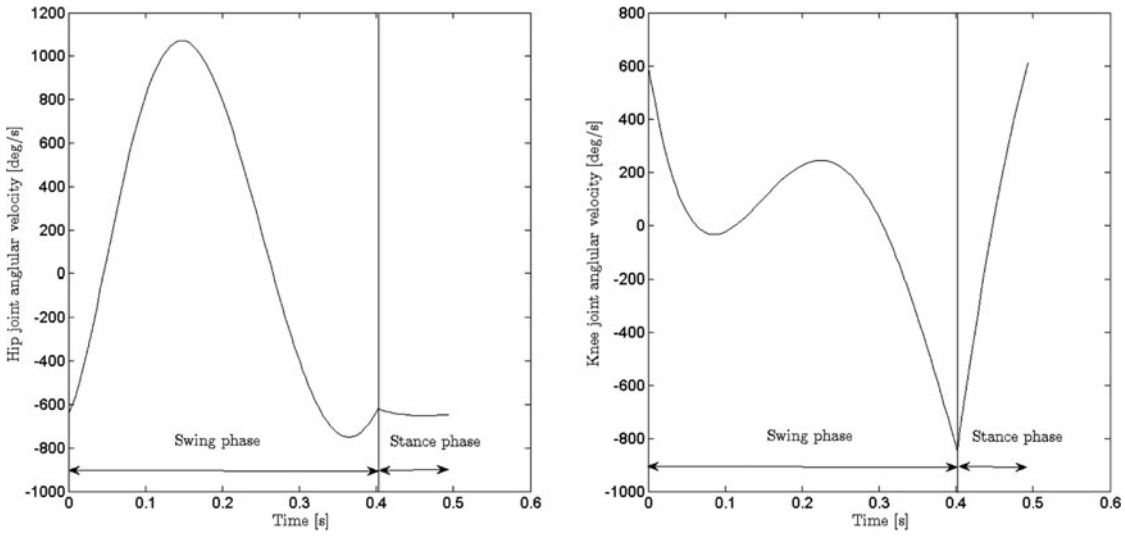

Fig. 9. Angular velocity of the actuated joints during one step.

duration of stance phase. A long jump distance requires large initial angular velocities for both joints at the beginning of the swing phase, which leads to large horizontal linear velocities.

The required torque for the actuated joints during one step is given in Fig. (11). Comparing the joint torque profiles in this case with those obtained for the torque-based optimization (Fig. (6)) shows that the two cases are notably different, particularly for the hip joint. Unlike the torque-optimized case, the hip torque for the velocity-optimized case does not require a sudden reverse at touch-down, due to the fact that the robot body tends to continue rotating in the same orientation after touch-down. The knee torque, however, requires a relatively large reverse torque at the beginning of the stance phase, indicating that it is preventing the spring to compress too much due to the high leg's momentum. During the spring extension, the knee actuator applies a negative torque to prevent the robot CoM from gaining too high a vertical linear velocity. Note that the impact torque for both joints at touch-down is still below the maximum values dictated by constraints (21)and (22). Figure (12) illustrates the ground reaction forces during the stance phase. For this case the highest ratio of the horizontal to vertical reaction forces occurs at the touch-down moment, and it is equal the 0.49. Hence, to avoid slippage the static friction coefficient between the toe and the ground surface must be larger than this

https://doi.org/10.1017/S0263574714002598 Published online by Cambridge University Press

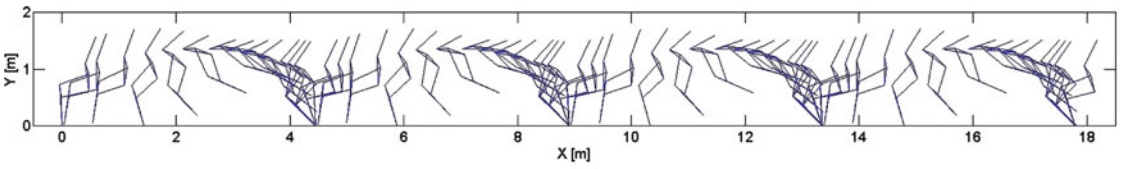

(a) Four steps of the motion

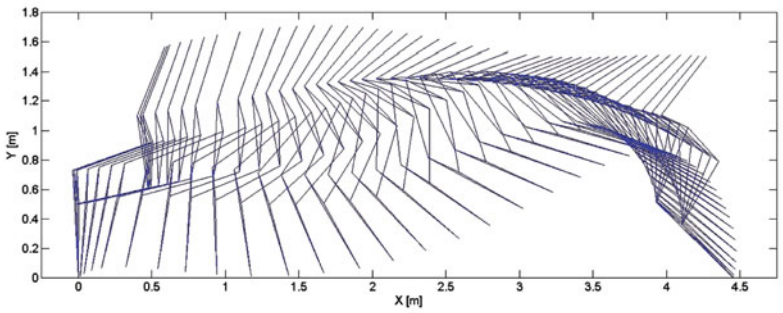

(b) Swing phase

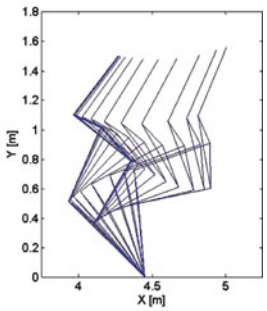

(c) Stance phase

Fig. 10. Stick diagram of the robot motion during each phase of motion. (a) Four steps of the motion. (b) Swing phase. (c) Stance phase.

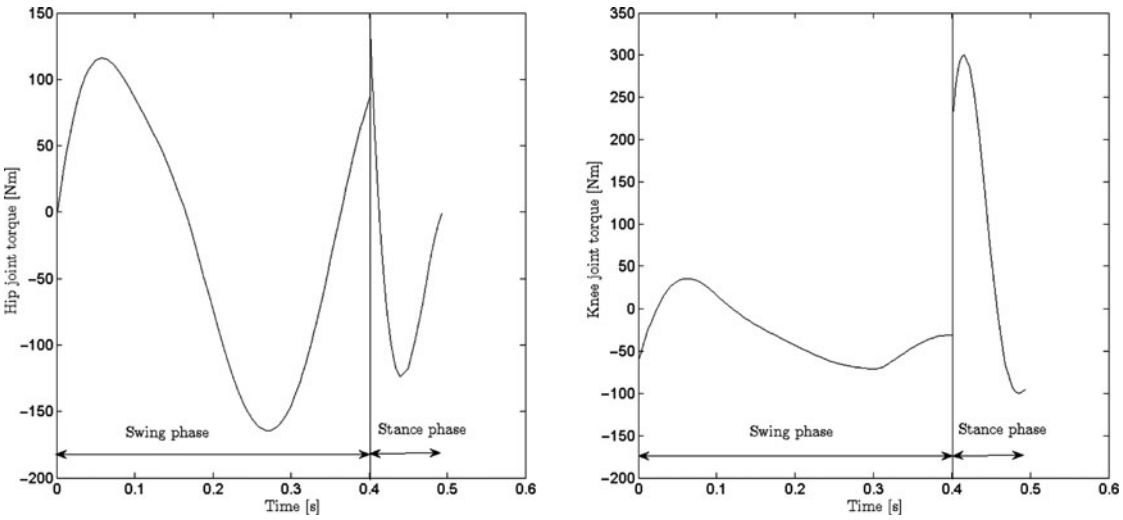

Fig. 11. Input torque of the actuated joints.

magnitude. This is feasible for typical surfaces. For example, the static friction coefficient of rubber on dry asphalt is in the range of 0.8–1.2.[26]

The optimization results for the minimum torque and maximum CoM velocity are given in the Table (III). In the table, the duty factor is the ratio of the duration of stance and swing phases. The leg length (L) is the length of the (imaginary) line connecting the hip to the toe $\{O_0O_3\}$. The leg angle is the angle between $\{O_0O_3\}$ and the horizontal line. The dimensionless speed β represents the normalization of the CoM horizontal velocity(u) for the leg length at touch-down (L_0), as defined in Eq. (30), and Froude number is the square of β.

$$\beta = \frac{u}{\sqrt{g.L_0}}. \tag{30}$$

https://doi.org/10.1017/S0263574714002598 Published online by Cambridge University Press

Table III. The leg variables for optimized motions.

Trajectory characteristic	Min. torque	Max. velocity
Swing phase duration [s]	0.4038	0.4026
Stance phase duration [s]	0.1788	0.0928
Step duration [s]	0.5826	0.4954
Leg length at touch-down L_0 [m]	1.287	1.22
Max CoM vertical displacement [m]	0.314	0.258
Max CoM horizontal displacement [m]	1.734	4.4283
Relative stride length	1.35	3.63
Average CoM horizontal velocity [m/s]	3.01	8.98
Leg angle at touch-down (angle of attack) [°]	74.41	65.9
Leg angle at lift-off [°]	100.93	110.06
Leg angle swept during stance phase [°]	26.52	44.16
Cumulative torque for one step [Nm]	908.1	1517.8
Duty factor	0.4428	0.2305
Dimensionless speed	0.85	2.59
Froude number	0.72	6.74

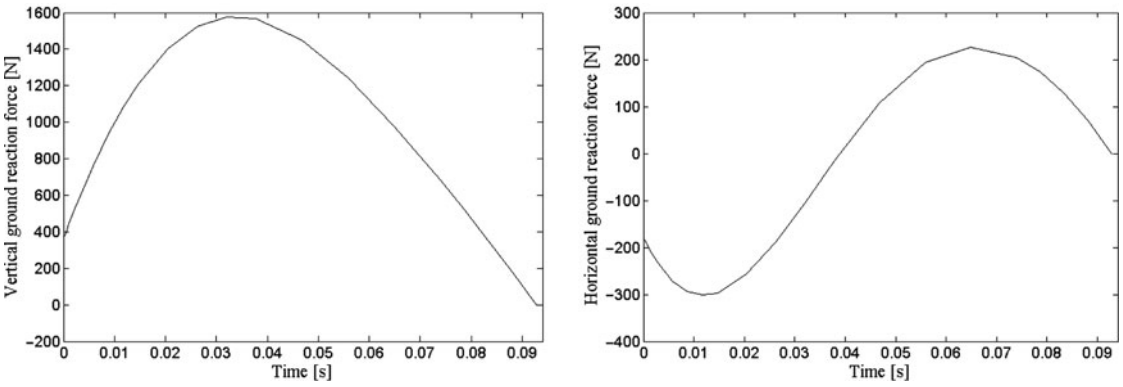

Fig. 12. Ground reaction forces during the stance phase.

The spring stiffness of the leg was kept the same in both minimum-torque and maximum-velocity optimizations. This is consistent with the experimental studies done by Farley *et al.*[27] indicating that in many animal species the leg stiffness remains mostly constant even when the forward velocity is increasing. Further, according to their measurements at the speeds near the mid-range of the trotting or hopping speed the duty factor for the animals under study (dog, horse, goat, red kangaroo and kangaroo rat) varies between 0.36 and 0.5. The measured dimensionless speed is between 1.1 and 1.8. They have concluded that since at these speeds the above-mentioned animals exhibit relatively similar values of both the duty factor and dimensionless speed, such speeds can be considered as physiologically equivalent, and the systems as dynamically similar. Interestingly from Table (III), the duty factor and dimensionless speed obtained from the minimum-torque optimization are close to the above-mentioned experimental results. This would indicate that the trotting or hopping gait in animals at physiologically equivalent speeds results in a minimum torque, thus energy, required for the motion. In addition, the experimental results in[27] show an increase in the angle swept by the leg during the stance phase with an increase in the forward velocity in the animals. Similarly, as shown in Table (III), the leg angle swept during stance phase also increases notably from minimum-torque to maximum-velocity optimized gaits.

In another relevant study,[28] the relationship between Froude number and the relative stride length, i.e., the horizontal distance travelled at each step per leg length is obtained for various quadrupeds. The study shows that for a Froude number close to 0.72, which is what was obtained from the minimum-torque optimization in this paper, the relative stride length is between 1.2 and 1.8, which is consistent with the optimization outcome. Similarly, for a Froude number of 6.74, which is the outcome of maximum-velocity optimization, the study shows that the relative stride length in quadrupeds is in

https://doi.org/10.1017/S0263574714002598 Published online by Cambridge University Press

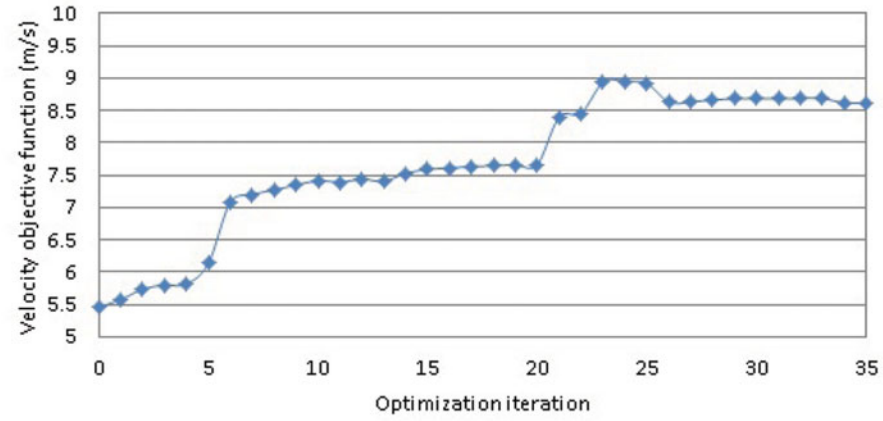

(a) Objective function

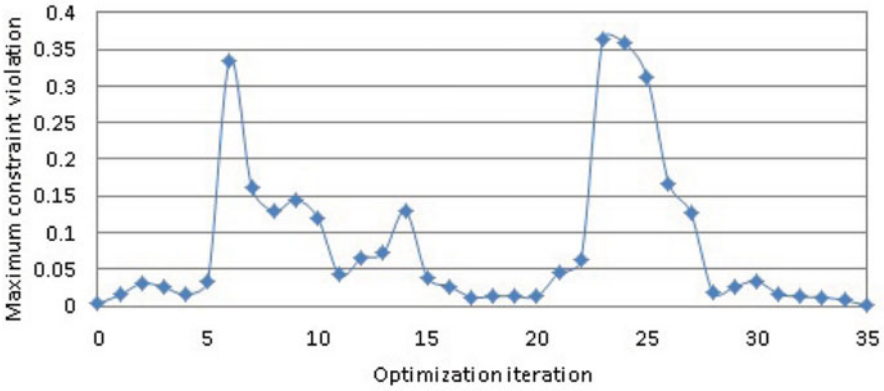

(b) Maximum constraint violation

Fig. 13. The performance of velocity-based optimization. (a) Objective function. (b) Maximum constraint violation.

the range of 3.1–4.3, which is again consistent with what was obtained from the maximum-velocity optimization in this paper.

Another interesting observation is about the leg angle at touch-down, which is also referred to as the leg angle of attack. Seyfarth *et al.*[29] investigated the dynamic parameters for a stable (hopping) motion of a simple passive SLIP model. They discovered that higher running/hopping velocities need either larger leg stiffness with a constant angle of attack or smaller angles of attack with a constant leg stiffness. This phenomenon has also been addressed in,[27] showing that in animals the angle of attack decreases with increase in the forward velocity. Since the leg stiffness in our case remains constant, increasing speed has resulted in decreasing the leg angle of attack, as shown in Table (III).

Lastly, Seyfarth *et al.*[29] also showed that running with a constant leg stiffness and angle of attack requires a minimum velocity. In our work, since there was no lower bound for the CoM velocity, obtaining a stable gait for a minimum torque is equivalent to having the lowest velocity and yet maintaining a cyclic motion. This was indeed verified by running the optimization for minimum CoM velocity, which resulted in the same gait as the one for the minimum-torque optimization. Therefore, the minimum hopping velocity for our case is 3.01[m/s] with a dimensionless speed of 0.85 and duty factor of 0.44. This minimum velocity is close to the gait transition velocity from walking to running in humans, which is measured to be around 2.3[m/s] with a dimensionless speed of 0.7 and duty factor of 0.4.[30,31]

To illustrate the overall performance of the optimization procedure, the variation of the objective function and the maximum constraint violation for the velocity-based optimization are shown in Fig. (13). The optimum solution is converged at nearly 56% of its initial value. The major challenge for the optimization appeared to be first with respect to constraints on minimizing the impact (Eqs. (11) and

https://doi.org/10.1017/S0263574714002598 Published online by Cambridge University Press

(12)) and then to those on the gait stability (Eqs. (9) and (10)). The optimum solution also resulted in the impact torque near the maximum value for the knee joint, indicating that a strong knee actuation is required for hopping at high speeds.

6. Conclusion

In this work, an optimization model was developed for designing various trajectories for the actuated joints of a hopping robot using a novel leg mechanism. Two dynamic models were derived for the robot during stance and swing phases. The optimization model includes the Bezier coefficients of joint trajectories as well as the initial conditions of the robot's gait as design parameters. Two objective functions were investigated to minimize the accumulative joint torque and maximize the robot's CoM velocity separately. Various constraints were defined for the optimization model to ensure continuous and cyclic motion for the robot. The results obtained from the optimizations were consistent with some investigations of running gaits in animal species. The developed optimization model can be used to study the effect of kinematic and dynamic parameters of the robot in the optimum gaits, which will be the next phase of this research. Further studies of system stability under disturbances must be performed while designing proper controllers to follow the optimum gait trajectories. As well, it is planned to implement the generated gait trajectories on a physical prototype of the four-bar linkage leg.

References

1. M. Raibert, "*Legged Robots that Balance*" (MIT press, Cambridge, MA., 1986).
2. M. Thompson and M. Raibert, "Passive dynamic running," *Lecture Notes Control Inf. Sci.* **139**, 74–83 (1990).
3. G. J. Zeglin, "Uniroo: A One-Legged Dynamic Hopping Robot" *BS Thesis* (Department of Mechanical engineering, MIT press, MA., 1991).
4. P. Gregorio, M. Ahmadi and M. Buehler, "Design, control, and energetics of an electrically actuated legged robot," *IEEE Trans. Syst. Man Cybern.* **27**, 626–634 (1997).
5. M. Ahmadi and M. Buehler, "Preliminary experiments with an actively tuned passive dynamic running robot," Experimental Robotics V, *Lect. Notes Control Inf.* **232**, 312–324 (1998).
6. M. Ahmadi and M. Buehler, "Controlled passive dynamic running experiments with the ARL-monopod II," *IEEE Trans. Robot.* **22**, 974–986 (2006).
7. S. H. Hyon, T. Emura and T. Mita, "Dynamics-based control of a one-legged hopping robot," *Proc. Inst. Mech. Eng. I: J. Syst. Control Eng.* 83–98 (2003).
8. T. Takahashi, M. Yamakita and S. H. Hyon, "An optimization approach for underactuated running robot," *SICE-ICASE International Joint Conference* (2006) pp. 3505–3510.
9. J. Vermeulen, D. Lefeber and B. Verrelst, "Control of foot placement, forward velocity and body orientation of a one-legged hopping robot," *Robotica* **21**, 45–57 (2003).
10. J. Vermeulen, "Trajectory generation for planar hopping and walking robots: An objective parameter and angular momentum approach" *Ph.D. Dissertation*, Department of Mechanical engineering (Vrije Universiteit Brussel, Brussels, 2004).
11. Q. Guo, C. J. B Macnab and J. K. Pieper, "Hopping on even ground and up stairs with a single articulated leg," *J. Intell. Robot. Syst.* **53**(4), 331–358 (2008).
12. Q. Guo, C. J. B Macnab and J. K. Pieper, "Generating efficient rigid biped running gaits with calculated take-off velocities," *Robotica* **29**, 627–640 (2010).
13. I. Poulakakis and J. W. Grizzle, "The spring loaded inverted pendulum as the hybrid zero dynamics of an asymmetric hopper," *IEEE Trans. Autom. Control* **54**, 1779–1793 (2009).
14. J. W. Hurst and A. Rizzi, "Series compliance for an efficient running gait," *IEEE Robot. Autom. Mag.* **15**, 42–51 (2008).
15. K. Sreenath, H. W. Park, I. Poulakakis and J. W. Grizzle, "A compliant hybrid zero dynamics controller for stable, efficient and fast bipedal walking on MABEL," *Int. J. Robot. Res.(IJRR)* **30**(9), 1170–1193 (2011).
16. T.-Y. Wu, T. J. Yeh and B.-H. Hsu, "Trajectory planning of a one-legged robot performing a stable hop," *Int. J. Robot. Res.* **30**(8), 1072–1091 (2011).
17. V. Ragusila and M. R. Emami, "A novel robotic leg design with hybrid dynamic," *J. Adv. Robot.* **27**(12), 919–931 (2013).
18. V. Ragusila and M. R. Emami, "Modelling of a robotic leg using bond graphs," *Simul. Modelling Pract. Theory* **40**, 132–143 (2014).
19. J. Pratt and R. Tedrake, *"Velocity based stability margins for fast bipedal walking,"* First Ruperto Carola Symposium in the International Science Forum of the University of Heidelberg entitled *"Fast Motions in Biomechanics and Robots"* (Heidelberg, Germany, 2005).

https://doi.org/10.1017/S0263574714002598 Published online by Cambridge University Press

20. M. Popovic, A. Goswami and H. Herr, "Ground reference points in legged locomotion: Definitions, biological trajectories and control implications," *Int. J. Robot. Res.* **24**(12), 1013–1032 (2005).
21. A. Seyfarth, H. Geyer and H. Herr, "Swing-leg retraction: A simple control model for stable running," *J. Exp. Biol.* **206**, 2547–2555 (2003).
22. M. Wisse, C. G. Atkeson and D. K. Kloimwieder, "Swing Leg Retraction Helps Biped Walking Stability," *Proceedings of 5th IEEE-RAS International Conference on Humanoid Robots* (2005) pp. 295–300.
23. E. R. Westervelt, J. W. Grizzle, C. Chevsllereau, J. H. Choi and B. Morris, *Feedback Control of Dynamic Bipedal Robot Locomotion* (Boca Raton: CRC Press, New York, 2007).
24. C. Chevallereau, G. Bessonnet, G. Abba and Y. Aoustin, *Bipedal Robots: Modelling, Design and Walking Synthesis* (Wiley, New York, 2009).
25. S. Tzafestas, M. Raibert and C. Tzafestas, "Robust sliding-mode control applied to a 5-link biped robot," *J. Intell. Robot. Syst.* **15**, 67–133 (1996).
26. P. J. Blau, *Friction Science and Technology from Concepts to Applications* (STLE: CRC Press, New York, 2009).
27. C. T. Farley, J. Glasheen and T. A. McMahon, "Running springs: Speed and animal size," *J. Exp. Biol.* **185**, 71–86 (1993).
28. R. M. Alexnader and A. S. Jayes, "A dynamic similarity hypothesis for the gaits of quadrupedal mammals," *J. Zool.* **201**, 135–152 (1983).
29. A. Seyfartha, H. Geyera, M. Gnthera and R. Blickhana, "A movement criterion for running," *J. Biomech.* **35**, 649–655 (2002).
30. A. Thorstensson and H. Roberthson, "Adaptations to changing speed in human locomotion: Speed of transition between walking and running," *Acta Physiol. Scand.* **131**(2), 211–214 (1987).
31. R. M. Alexander, "Optimization and gaits in the locomotion of vertebrates," *Physiol. Rev.* **69**(4), 1199–1227 (1989).

Appendix: The explicit relation between angles θ_3, θ_5 and θ_2

Writing the kinematic equations in the closed system of $\{O_1O_2O_5O_4\}$ and in the coordinate system of $\{x_4, y_4\}$ shown in Fig. (1), gives:

$$a_2\cos(\theta_2-\phi_1)+a_6\cos(\theta_3+\theta_2-\phi_3-\phi_1)=a_7\cos(\phi_4)+a_5\cos(\theta_5),$$
$$a_2\sin(\theta_2-\phi_1)+a_6\sin(\theta_3+\theta_2-\phi_3-\phi_1)=a_7\sin(\phi_4)+a_5\sin(\theta_5),$$

solving these equations for θ_3 and θ_5 results in:

$$\theta_3=\arccos\left(\pm a_5\sqrt{\frac{1-K^2}{t^2+s^2}}\right)-\arctan(s/t)-\theta_2+\phi_3+\phi_1,$$
$$\theta_5=\arccos\left(\pm a_6\sqrt{\frac{1-K^2}{t^2+s^2}}\right)-\arctan(s/t),$$

where

$$K=\frac{{a_6}^2+{a_5}^2-s^2-t^2}{2.a_6.a_5},$$
$$s=a_2\cos(\theta_2-\phi_1)-a_7\cos(\phi_4),$$
$$t=a_2\sin(\theta_2-\phi_1)-a_7\sin(\phi_4).$$

Differentiating the above kinematic equations with respect to θ_2 and solving for the $\frac{\partial\theta_3}{\partial\theta_2}$ and $\frac{\partial\theta_5}{\partial\theta_2}$, gives:

$$d_{3,2}=\frac{\partial\theta_3}{\partial\theta_2}=\frac{a_2}{a_6}.\frac{\sin(\theta_5-\theta_2+\phi_1)}{\sin(\theta_3+\theta_2-\theta_5-\phi_3-\phi_1)}-1,$$
$$d_{5,2}=\frac{\partial\theta_5}{\partial\theta_2}=\frac{a_2}{a_5}.\frac{\sin(\theta_3-\phi_3)}{\sin(\theta_3+\theta_2-\theta_5-\phi_3-\phi_1)}.$$

https://doi.org/10.1017/S0263574714002598 Published online by Cambridge University Press